On the Equalization of an OFDM-Based Radio-over-Fiber System Using Neural Networks

Leila SAFARI [1], Gholamreza BAGHERSALIMI [1], Ali KARAMI [1], Abdolreza KIANI [2]

[1]Dept. of Electrical Engineering, University of Guilan, Rasht, Iran,
[2] Dept. of Electrical Engineering, Abadan Branch, Islamic Azad University, Abadan, Iran

leila_safari_81@yahoo.com, bsalimi@guilan.ac.ir, karami_s @guilan.ac.ir, ab2rezakiani@yahoo.com

Submitted May 29, 2016 / Accepted November 23, 2016

Abstract. *In this study the impact of a Radio-over-Fiber (RoF) subsystem on the performance of Orthogonal Frequency Division Multiplexing (OFDM) system is evaluated. The study investigates the use of Multi-Layered Perceptron (MLP) and Radial Basis Function (RBF) neural networks to compensate for the optical subsystem nonlinearities in terms of bit error rate, error vector magnitude, and computational complexity. The Bit Error Rate (BER) and Error Vector Magnitude (EVM) results show that the performance of MLP neural network is superior to that of RBF neural network and time-multiplexed pilot-based equalizer especially in the case of highly nonlinear behavior of the RoF subsystem.*

Keywords

Radio-over-Fiber, OFDM, equalization, neural network, RBF, MLP, BER, EVM

1. Introduction

In recent years, with the growth of technologies, efficient high-speed data transmission techniques over wireless channels have become important topics for research. A key enabling technology supporting the provision of cellular communications is Radio-over-Fiber (RoF), alternatively known as Hybrid Fiber Radio (HFR). This technology combines two media: radio and optical. Typically, the optical part is used to interconnect a central radio processing facility with a remote radio antenna, the latter providing coverage to wireless broadband users. Some of the advantages offered by a RoF system include low signal attenuation (in the fiber), improved coverage and system performance, enhanced capacity, low Radio Frequency (RF) power dissipation, reduced complexity due to the centralized processing of RF signals and ultimately low system costs [1–3]. However, the performance of RoF systems can be severely affected by nonlinear effects in the transmission channel. In the RF part of a RoF system, the main source of nonlinearity is the power amplifier. In the optical part of a RoF system, the main sources of nonlinearity include the laser-diode (LD) light source, the optical fiber and the PIN photo detector (PD). For short haul optical links, the fiber nonlinearity is usually small and can be neglected from system considerations. Also, the PD can be assumed to be linear for the same conditions.

One area of interest in modern communications is Orthogonal Frequency Division Multiplexing (OFDM) which is becoming widely used in wireless communication systems due to its high data rate transmission capability with high bandwidth efficiency and also its robustness to multipath fading without requiring complex equalization techniques [2, 4]. OFDM has been adopted in a number of wireless applications including Digital Audio Broadcast (DAB), Digital Video Broadcast (DVB), Wireless Local Area Network (WLAN) standards such as IEEE 802.11g and Long Term Evolution (LTE) [4, 5]. To mitigate ISI (inter-symbol interference) introduced by the channel, a Cyclic Prefix (CP) is used which in turn leads to spectral inefficiency [4]. In comparison to single carrier systems including code division multiple access (CDMA) systems, more vulnerability to nonlinearity, frequency offset due to fading etc., and phase noise are OFDM disadvantages [4], [6], [7].

Channel estimation is a subject which has received a great deal of attention by researchers in recent years. In wireless systems, channel estimation techniques are used for the estimation of RF channel impulse response (CIR) in order to compensate for the amplitude distortion and phase rotation introduced by the RF channel variations. In cellular communication, estimation is achieved by time-multiplexed pilot signals, code-multiplexed pilot signals or a combination of these signals [8]. In the wireless local area network (LAN) systems, on the other hand, estimation is carried out by frequency (subcarrier) multiplexed pilot signals, time (symbol) multiplexed pilot signals or a combination of these signals [4]. All such equalization techniques require extra hardware at either the transmit and/or the receive side of the communication link. To compensate for RF channel impairments, two basic one-dimensional (1-D) estimation techniques namely the block-type (time-multiplexed) and comb-type (frequency-multiplexed) along with some combinations of both schemes (scattered-type) are employed in OFDM systems [4]. Normally, the aforementioned techniques are used to estimate and compensate for fading channels.

Neural networks (NNs) have been evolved into a powerful tool in solving complex applications such as function approximation, nonlinear classification, nonlinear system identification, nonlinear mapping between the high-dimensional input and output spaces, and forming complex decision regions with nonlinear decision boundaries [9–16]. Further, because of the nonlinear characteristics of the NNs, these networks have been found successful in channel estimation and equalization in digital communication systems. In [13], a method for channel estimation and equalization based on the multi-layered perceptron (MLP) neural network was presented, which resulted in a robust solution. Radial basis function (RBF), as another NN scheme, was also used for channel equalization [10, 14].

For RoF-OFDM communications, there is a dearth of publications in the context of channel estimation and compensation [11, 17]. In particular, the effectiveness of all methods has not been substantially investigated before. Further, as will be shown, the system performance can be improved by using neural networks. It should be emphasized that both the amplitude and phase distortions of an optical channel affect the system performance. Also, due to the hysteresis-type memory of the optical subsystem, the entire RoF link suffers more from the phase impairments and frequency-dependent nonlinearities when compared to other nonlinear elements.

In this paper, the impact of the optical subsystem nonlinearities on the performance of an OFDM system (adopted from IEEE802.11g standards [18]) is studied with respect to the channel estimation and equalization functions using both the MLP and the RBF neural networks. The results for the OFDM system Bit Error Rate (BER), Error Vector Magnitude (EVM), and computational complexity performances are presented for different modulation schemes, neural networks, and Output Back-off (OBO) levels when two neural networks are used to compensate for the distortion introduced by both of the optical channel and the RF channel. Strictly speaking, the overall subsystem that is, the optical (nonlinear) subsystem and the RF channel (represented by AWGN – additive white Gaussian noise) is estimated and equalized using two different neural networks under different conditions. Further, the effectiveness of the proposed MLP NN and RBF NN-based approaches is compared with that of the (time-multiplexed) pilot-based equalizer. Also, as this research focuses only on the optical subsystem, other sources of nonlinearity, such as the RF High Power Amplifier (HPA), are not considered. Finally, for the sake of simplicity and focusing on the equalization of the nonlinear subsystem, operations such as coding and interleaving along with fading channel are not considered.

The rest of the paper is organized as follows. Section 2 introduces the theoretical background and system model for estimating and equalizing the optical subsystem. Section 3 presents the MLP and RBF NN structures for cannel equalization while the results of neural network-based equalization are presented in Sec. 4. Finally, Section 5 concludes the paper.

2. Description of the RoF-OFDM System

In this section, the mathematical description of the baseband RoF-OFDM system for transmission of one OFDM symbol is presented. Figure 1 shows the block diagram of the RoF-OFDM communication system employing a NN-based equalizer. Also, various data and signals are labeled properly. In general, this model consists of a transmitter, an optical subsystem, a RF channel and a receiver. These subsystems are explained in the following subsections.

2.1 Transmitter

RoF-OFDM transmitter consists of a random digital data generator and an OFDM modulator. This transmitter sends its data bit stream $\{a_k\}$ to the modulator where they are translated to a symbol train using the Quadrature Amplitude Modulation (QAM) mapping rule. Let the user signal over the OFDM block T be denoted by

$$x_{\mathrm{D}}(t) = \sum_{n=0}^{N_s-1} D_n \,\delta(t - nT_{\mathrm{s}}); \qquad 0 \le t \le T \tag{1}$$

where $D_n = b_n + \mathrm{j}d_n$ is the n-th (baseband) data symbol, b_n is the in-phase component of the n-th data symbol, d_n is the quadrature component of the n-th data symbol, T_{s} is the data symbol duration, N_{s} is the number of data symbols being transmitted in the OFDM symbol (block) period $T = N_{\mathrm{s}} \cdot T_{\mathrm{s}}$, and $\delta(t)$ is the Dirac delta function. The serial stream of data symbols is first converted into N parallel streams. An inverse DFT (Discrete Fourier Transform) is taken on each set of data symbols, giving a set of complex time-domain values. Then, a Cyclic Prefix (CP) is prepended in order to compensate for the Inter-symbol Interference (ISI). Thus, the OFDM symbol $x(t)$ is given by [4]

$$x(t) = \sum_{k=-k_1}^{N_{\mathrm{s}}} \sum_{n=0}^{N_s-1} D_n \exp\left(\mathrm{j}2\pi \frac{n}{N_{\mathrm{s}}}\right); \quad -\frac{k_1 T}{N_{\mathrm{s}} + k_1} < t < \frac{N_{\mathrm{s}} T}{N_{\mathrm{s}} + k_1} \tag{2}$$

where k_1 is the CP length. Also, the OFDM signal can be described by

$$x(t) = r(t)\exp(j\theta(t)) \tag{3}$$

where $r(t)$ and $\theta(t)$ are the amplitude and phase of the transmit signal, respectively.

2.2 Optical Subsystem

It is customary in communication systems to analytically describe the system performance provided that the analytic model for all components/subsystems (i.e. input-output relationship) are available. Beside validity under certain circumstances and difficulty in mathematical operations, some physical problems cannot be described by mathematical models. In such cases behavioral modeling is used in such a way that the system is treated as a black box

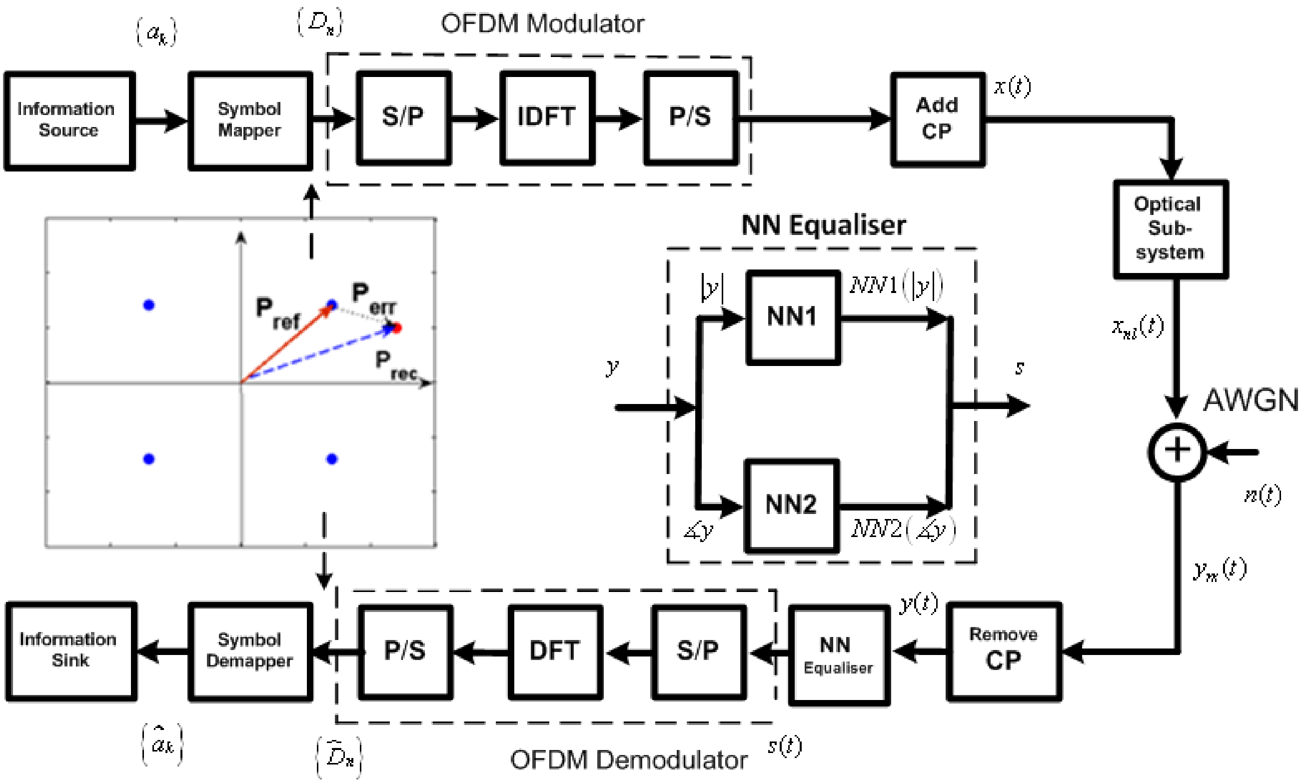

Fig. 1. Block diagram of a NN equalizer for a RoF-OFDM system.

whose characteristics are represented by the so called transfer functions or alternatively the large-signal response. These functions are expressed as AM-AM (amplitude-to-amplitude) and AM-PM (amplitude-to-phase) characteristics. It must be emphasized the all deficiencies in the system (such as optical noise and static and dynamic nonlinearities in the optical subsystem's case) are included in the black box model. The main advantage of behavioral modeling is that it can describe a complex system with no need to a thorough knowledge of its subsystems.

When the envelope of the signal is varying slowly, the large signal response can be used instead of the instantaneous value of the signal. The AM-AM/PM characteristics are valid provided that the device "memory time" (amplitude - and frequency-dependent time delay between the transmitted and received RF signal) is much smaller than the reciprocal of the input signal bandwidth [18]. As a rule of thumb, the AM-AM/PM models are used when the memory time of the nonlinear system is at least twice less than the reciprocal of the envelope frequency [19, 20]. This criterion is satisfied in this research.

In this study, the optical subsystem (shown in Fig. 1) includes a laser diode (LD), a 2.2 km long single-mode fiber and a photodiode (PD) [3]. The radio frequency is 1.8 GHz, however the frequency response of the optical link (centred at 1310 nm) is flat over frequencies $1.7 < f < 2.2$ GHz. The AM-AM/PM transfer characteristics are depicted in Fig. 2. Moreover, a pictorial description of OBO is shown in Fig. 2 and is defined (on a logarithmic scale) as the difference between the maximum output power and the output power at the operating point.

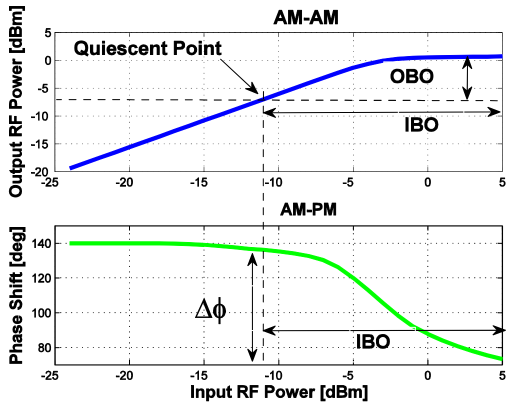

Fig. 2. AM-AM/PM characteristics (IBO: Input Back-off) [3].

The OFDM signal passes through the optical (nonlinear) subsystem whose output is described by

$$x_{\mathrm{nl}}(t) = G_{\mathrm{out}}\sqrt{\left(2R_{\mathrm{out}}^{-1}\right) f_{\text{AM-AM}}\left(0.5R_{\mathrm{in}}(G_{\mathrm{in}}|x(t)|)^2\right)} \\ \exp[\mathrm{j}f_{\text{AM-PM}}(0.5R_{\mathrm{in}}(G_{\mathrm{in}}|x(t)|)^2 + j\psi_{\mathrm{x}}(t)] \quad (4)$$

where IBO is the input back-off on a linear scale, $G_{\mathrm{in}} = \sqrt{\max\left(P_{\mathrm{RF},i}\right)/\left(IBO \cdot P_{\mathrm{m}}\right)}$ is the gain of the pre-amplifier which matches the output power of the transmit RRC filter to the input power of the optical subsystem [3], P_{m} is the maximum input RF power to the optical subsystem before the pre-amplifier, $\max(P_{\mathrm{RF},i})$ is the (measured) maximum input RF power before the pre-amplifier, $\psi_{\mathrm{x}}(t)$ is the phase of the signal $x_t(t)$, $R_{\mathrm{in}} = R_{\mathrm{out}} = 50\ \Omega$ is the input/output impedance of the optical subsystem, and G_{out} is a linear gain which sets the overall gain of the optical subsystem to unity. Also, $f_{\text{AM-AM}}(.)$ and $f_{\text{AM-PM}}(.)$ are the AM-AM and AM-PM transfer characteristics of the optical subsystem, respectively. To explicitly representing the amplitude and phase transfer characteristics of the optical subsystem, equation (4) can be written as

$$x_{\text{nl}}(t) = g\left[x_{\text{t}}(t)\right] = F\left[r(t)\right]\exp(\text{j}[\phi\left[r(t)\right] + \theta(t)]) \tag{5}$$

where g is a nonlinear function which represents the optical subsystem, and F and ϕ are known as AM-AM and AM-PM transfer functions, respectively.

2.3 RF Channel

The output signal of the optical subsystem is corrupted by a zero-mean complex Additive White Gaussian Noise (AWGN) process $n(t)$. So, the received signal is described by

$$y_{\text{rx}}(t) = x_{\text{nl}}(t) + n(t)\,. \tag{6}$$

Also, equation (5) can be rewritten by using

$$x_{\text{nl}}(t) = x_{\text{d}}(t) + n_{\text{d}}(t) \tag{7}$$

where $x_{\text{d}}(t)$ is the amplified/attenuated version of signal $x(t)$, and $n_{\text{d}}(t)$ is the total distortion introduced by the optical subsystem and AWGN channel. In addition, E_{b} is defined as the average bit energy of the user. So, the received signal can be described as

$$y_{\text{rx}}(t) = x_{\text{d}}(t) + n_{\text{d}}(t) + n(t)\,. \tag{8}$$

Then, the signal-to-interference-noise ratio ($SINR$) is given as follows

$$SINR = \frac{E[x_{\text{d}}^{\,2}(t)]}{E[n_{\text{d}}^{\,2}(t) + n^2(t)]}\,. \tag{9}$$

2.4 Receiver

The receiver consists of a NN equalizer to compensate for the channel impairments along with an OFDM demodulator. First, by removing the CP, the resultant signal is applied to the NN equalizer. The NN equalizer is composed of two sub-networks that compensate for the amplitude and phase of the transmitted signal. These sub-networks learn the knowledge of the channel by using the learning algorithm in the training phase. The output of the equalizer $s(t)$ is then compared with the transmit signal $x(t)$ to produce an error which is used to update the weights of the network in the training phase. Then, during system normal operation phase these sub-networks recover the amplitude and phase of signal $x(t)$. Following amplitude estimation and phase derotation of the received signal, the resultant serial data are converted into parallel, and a DFT is taken followed by a conversion to serial data whose output is denoted by $\{\hat{D}_n\}$. These serial data are then demodulated using 4/16QAM demapping rule. Finally the resultant bit stream $\{\hat{a}_k\}$ is compared with the transmit one i.e. $\{a_k\}$.

3. Neural Network Model for Channel Equalization

In this paper, two NN structures i.e. MLP and RBF are employed for channel estimation and equalization. These are described as follows.

Figure 3 shows the proposed MLP structure. In these configurations, I and J denote the number of neurons in the input and hidden layers, respectively. The proposed NN comprises two sub-networks NN1 and NN2 that estimate and compensate for the amplitude and phase of the transmitted signal x, respectively. The MLP NNs are usually trained in a supervised manner with a highly popular algorithm known as the error back-propagation (BP). However, the conventional back-propagation method is often too slow for many practical problems; thus, in this paper the *resilient* back-propagation technique, which is one of the fast training algorithms, is employed to accelerate the training process [21]. The system error is computed between the target outputs and the corresponding estimated outputs by the NN. The weights associated with the NN are then updated using the BP algorithm [13]. This procedure is continued till the Mean-Square Error (MSE) of the NN reaches a predetermined value.

Figure 4 shows the proposed RBF NN structure where m and n denote the number of neurons in the input and hidden layers, respectively. In the hidden layer, the input space is expanded onto a higher dimensional space by applying a nonlinear transformation using a set of RBFs. At the output layer, linear combinations of the outputs produced in the hidden layer neurons are calculated in order to obtain the RBF network final outputs [15]. The output of the network is represented by:

$$y(x) = \sum_{i=1}^{N} w_i \phi_i(x) \tag{10}$$

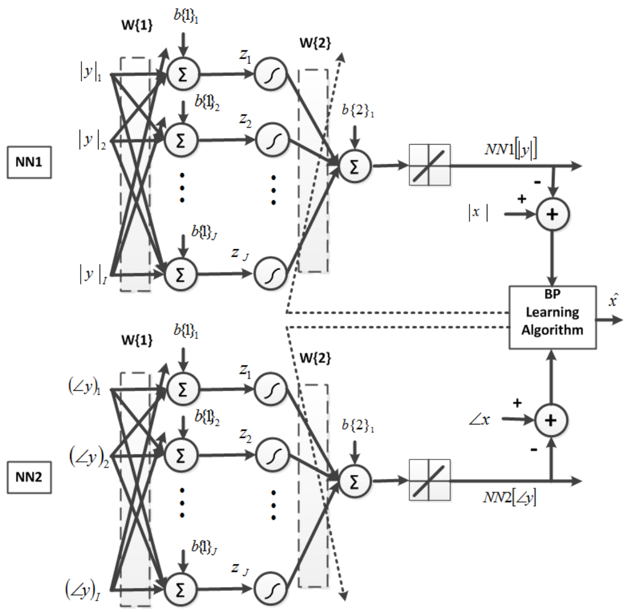

Fig. 3. The proposed MLP neural network to compensate for amplitude (top) and phase (bottom) distortions.

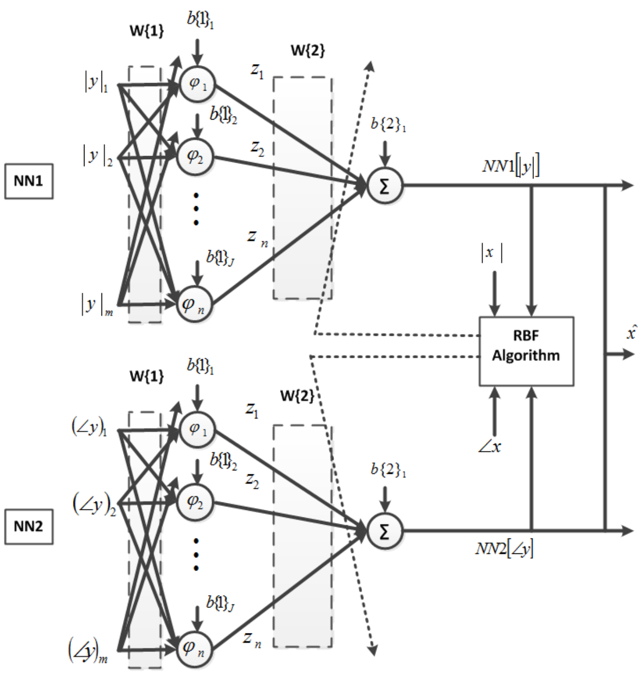

Fig. 4. The proposed RBF neural network to compensate for amplitude (top) and phase (bottom) distortions.

where x is the input vector and w_i's are the weight values corresponding to the output layer. A Gaussian basis function is usually used for the hidden neurons which is given by:

$$\phi(x) = \exp\left(-\frac{\|x-c\|^2}{\sigma^2}\right) \tag{11}$$

where c is the center of the Gaussian function and σ is the spread parameter. Training of an RBF network is accomplished by obtaining suitable centers for the hidden layer neurons along with appropriate weight values for the output layer. In the training phase of an RBF-NN, the centers and spread parameters of the hidden layer neurons along with weights for the output layer neurons are usually determined by employing unsupervised and supervised training algorithms, respectively.

The sub-networks in both MLP and RBF NNs are trained using the same training sequence. The outputs of NN1 and NN2 in the case of MLP NN are given by

$$\begin{aligned} NN1\left[|y(t)|\right] &= f_2\sum_{i=1}^{J} c_{1i} f_1[w_{1i}\,|\,y(t)\,|+b_{1i}], \\ NN2\left[\angle y(t)\right] &= f_2\sum_{i=1}^{J} c_{2i} f_1[w_{2i}(\angle y(t)) + b_{2i}] \end{aligned} \tag{12}$$

where $f_1(.)$ is a sigmoid function used for hidden layer neurons, $f_2(.)$ represents the linear activation function used for output layer neurons, $\{w_{1i}, c_{1i}, b_{1i}\}$ and $\{w_{2i}, c_{2i}, b_{2i}\}$ are the weights and biases corresponding to the NN1 and NN2, respectively. Also, J is the number of neurons in the hidden layer. The outputs of NN1 and NN2 in the case of RBF NN are given by

$$\begin{aligned} NN1[|\,y(t)\,|] &= a_{10} + \sum_{k=1}^{n} a_{1k}\varphi_k(|\,y(t)\,|), \\ NN2[\angle y(t)] &= a_{20} + \sum_{k=1}^{n} a_{2k}\varphi_k(\angle y(t)) \end{aligned} \tag{13}$$

where φ_k represents the Gaussian function used for the k-th hidden layer neuron, a_{1k} and a_{2k} are the weights connecting the k-th hidden unit to the output unit in the NN1 and NN2 sub-networks. In addition, a_{10} and a_{20} are respectively the bias terms used in the NN1 and NN2 sub-networks, and n represents the number of hidden neurons in the two sub-networks.

After training, both trained NNs are ready to produce an estimate for the transmitted signal $\hat{x}$, which can be shown by (14)

$$\hat{x}(t) = NN1\left[|y(t)|\right]\exp\left(\mathrm{j}NN2\left[|\angle y(t)|\right]\right). \tag{14}$$

4. Results and Discussion

To assess the impacts of the optical subsystem on OFDM in the presence of nonlinearity, computer simulations were performed based on the system model shown in Fig. 1. A key performance metric for modern communication systems is EVM (in dB), which is defined as [5]

$$EVM\,(\mathrm{dB}) = 10\log_{10}\left(\frac{P_{\mathrm{err}}}{P_{\mathrm{ref}}}\right) \tag{15}$$

where P_{err} is the RMS (Root-Mean Square) power of the error (due to nonlinear time-variant channel) vector and P_{ref} is the reference constellation average power in the I (in-phase)-Q (quadrature) plane (see Fig. 1).

To enable statistically valid simulation results in reasonable simulation times, Monte-Carlo methods are used during the simulation. Also, the OFDM system parameters [18] and optical subsystem parameters [3] are summarized in Tab. 1.

DFT size (Number of subcarriers)	64
Data modulation	4/16QAM
OBO [dB]	0, 0.2, 0.5, 3
Number of input neurons	20
Number of hidden neurons in MLP-NN	65
Number of hidden neurons in RBF-NN(Number of epochs)	1 000
Number of epochs for training RBF-NN	1 000
Number of output neurons	1
Number of training bits	40 000
Total bits sent	10 000 000
Number of bits per block	800
Number of pilot bits per block (for the 1-D time-multiplexed case)	80 (10 % of the total power)

Tab. 1. Simulation parameters.

The estimation for both NNs by using 4/16QAM modulation schemes is achieved individually. In addition, the performance of a time-multiplexed (block type) pilot-aided equalizer is evaluated to compare with the results obtained by the NNs. Table 1 shows the simulation parameters used in this study.

Now, the performance of the proposed NN-based equalizers is discussed in terms of BER, EVM, and computational complexity.

4.1 BER Performance

Bit error rate was carried out for different values of OBO using 4QAM and 16QAM modulation schemes. The BER results obtained by the proposed NNs are compared with those of the pilot-aided estimation. BER curves for different E_b/N_0 values are shown at different OBO values. Figures 5 and 6 show the BER performance of the system in the presence of AWGN for four OBO values, i.e. 0 dB (the worst case scenario), 0.2 dB, 0.5 dB, and 3 dB (the best case scenario) with 4QAM and 16QAM signal constellations, respectively. From the plots we observe that by increasing the nonlinearity of the optical subsystem (i.e., decreasing the OBO value) the MLP NN-based equalizer performs more efficiently than the pilot-aided equalizer. Upon a closer observation, we also note that the MLP NN performs better than the RBF NN and the pilot-based estimators. These observations confirm that the optical subsystem was estimated more efficiently by the trained MLP neural network in comparison to the pilot-based estimator.

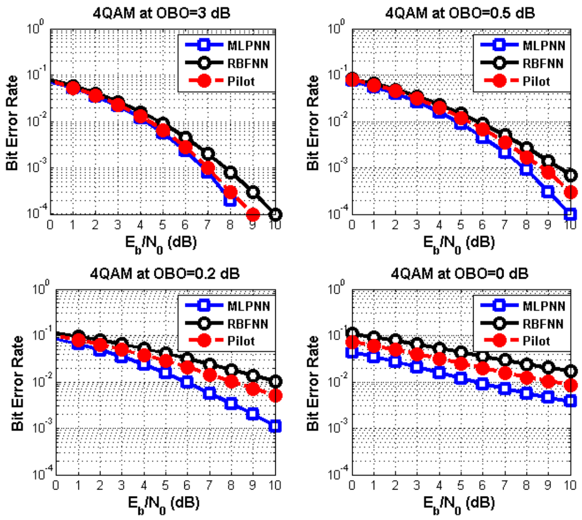

Fig. 5. BER for RoF-OFDM-4QAM at *OBO* = 3 dB (top left), *OBO* = 0.5 dB (top right), *OBO* = 0.2 dB (bottom left), and *OBO* = 0 dB (bottom right).

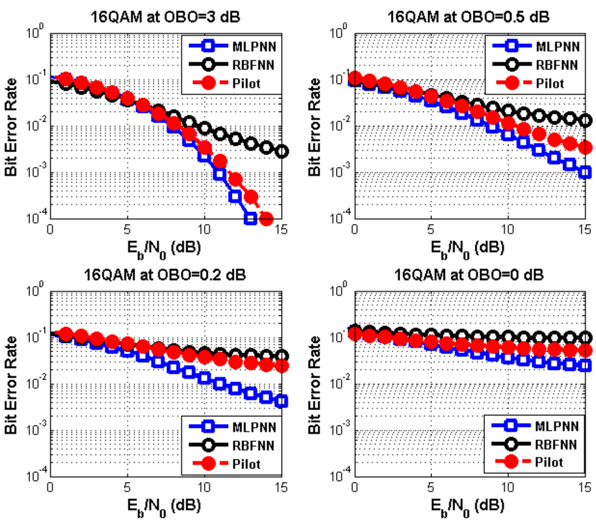

Fig. 6. BER for RoF-OFDM-16QAM at *OBO* = 3 dB (top left), *OBO* = 0.5 dB (top right), *OBO* = 0.2 dB (bottom left), and *OBO* = 0 dB (bottom right).

4.2 EVM Performance

EVM is a measure used to quantify the performance of a digital radio transceiver. A signal sent by an ideal transmitter would have all constellation points precisely at the ideal locations (see Fig. 1 for the 4QAM case). However, various imperfections in the implementation such as carrier leakage, phase noise, nonlinearity etc. cause the actual constellation points to deviate from the ideal locations. Informally, EVM is a measure of how far the points are from the ideal locations. In this subsection, the EVM is carried out for different OBO values given in Tab. 1. Figures 7 and 8 show the EVM performance for different E_b/N_0 values and two extreme OBO values, i.e., 0 and 3 dB, respectively.

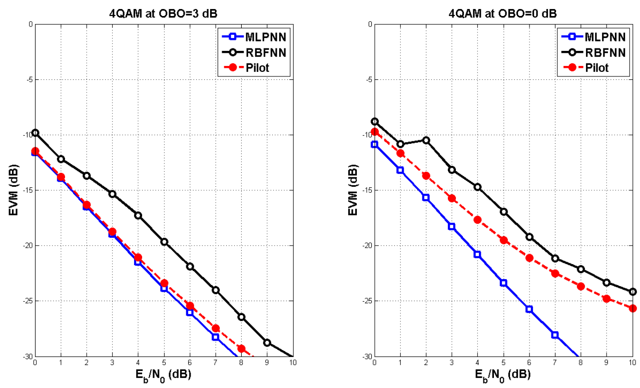

Fig. 7. EVM for RoF-OFDM-4QAM at *OBO* = 3 dB (left) and *OBO* = 0 dB (right).

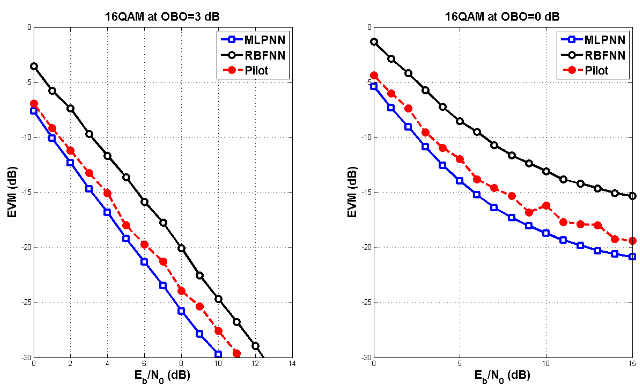

Fig. 8. EVM for RoF-OFDM-16QAM at *OBO* = 3 dB (left) and *OBO* = 0 dB (right).

The EVM performance of the NNs is compared with each other and with that of the pilot-aided estimator. It is clear that the EVM curve for the MLP NN is superior (lower) than EVM curves for the RBF and pilot-based equalizers. Therefore, the MLP NN has better performance in collecting the actual constellation points around their ideal locations in comparison to the other equalizers. It is also observed that the MLP NN performs more efficiently than the pilot-aided equalizer and RBF-based equalizer in the linear and nonlinear regions of the optical subsystem.

4.3 Computational Complexity

Table 2 compares the required computational parameters for 1 000 iterations of training in both types of NNs and modulation schemes. In MLP and RBF networks, the number of nodes in the input layer is 20, the number of neurons in the hidden layer in the MLP NN is 65, and one neuron in the output layer is considered for both NNs. To analyze the performance of NNs, each equalizer is trained for 1 000 epochs, and then the hidden neurons in the RBF NN are increased to 1 000. The number of training symbols is 40 000 for all NNs and it can be seen from Tab. 2 that the RBF NN requires an additional division and exp(.) operation because of using a Gaussian basis function as given by (11). In addition, since in the RBF NN the input space is mapped onto a high dimensional space, its computational complexity is higher than that of the MLP NN. Besides, the elapsed times for performing 1 000 epochs of training for 4QAM and 16QAM schemes on a core (TM) 2 Duo CPU with 2.67 GHZ and 4 GB RAM were, respectively, 156 seconds and 230 seconds for the case of the MLP NN, while they were 1052 seconds and 1095 seconds for the case of RBF NN. Therefore, it can be concluded that the training time for the MLP NN is shorter than that of the RBF NN.

Number of	**MLP**		**RBF**	
Weights	φ_1	1431	$n(m+k)$	21000
Additions	$3\varphi_2 + 3K - IJ$	2798	$2mn + m + n + k$	41021
Multiplications	$4\varphi_2 + 3\varphi_3 + 2K - IJ$	4420	$m\,n + m + 2n + k$	22021
tanh(.)	φ_3	86	----	----
Division	----	----	$m + n$	1020
Exp(.)	----	----	n	1000
$\varphi_1 = (I+1)J + (J+1)K,\ \varphi_2 = IJ + JK,\ \varphi_3 = I + J + K$				

Tab. 2. Comparison of computational complexity.

5. Conclusion

In this paper, a neural network (NN)-based equalizer was proposed for estimation and equalization of the optical subsystem effects in an OFDM-based RoF communication system. Two different NNs were trained considering two modulation schemes, and their testing results were compared. It was shown that the MLP NN could estimate and compensate for the subsystem effects more efficiently than the RBF NN. The comparison was achieved in terms of BER and EVM for a range of E_b/N_0 values. The simulation results corresponding to different linear and nonlinear behaviors of the subsystem confirmed the superiority of the MLP NN-based equalizer in estimating the (optical) channel behavior over the RBF NN-based equalizer in terms of EVM, BER, and computational complexity. It was also shown that an MLP-NN with a proper architecture could be trained in a shorter time compared to the RBF-NN. Finally, a comparison of the proposed NN-based equalizer with a pilot-based estimator revealed that the MLP-based equalizer had a better performance compared to the pilot-based equalizer.

Acknowledgments

The authors would like to thank the anonymous reviewers for their helpful comments that helped to improve this paper considerably.

References

[1] AL-RAWESHIDY, H., KOMAKI, S. *Radio-over-Fibre Technologies for Mobile Communications Networks*. Artech House, 2002. ISBN: 978-1580531481

[2] FERNANDO, X. N. *Radio over Fiber for Wireless Communications: From Fundamentals to Advanced Topics*. John Wiley and Sons, 2014. ISBN: 978-1-118-79706-8

[3] FERNANDO, X. N., SEASAY, A. B. Characteristics of directly modulated RoF link for wireless access. In *Proceeding of Canadian Conference on Electrical and Computer Engineering CCECE 2004*. Niagara Falls (Canada), 2004, vol. 4, p. 2167–2170. DOI: 10.1109/CCECE.2004.1347673

[4] SHEIKH BAHAI, A. R., SALTZBERG, B. R., ERGEN, M. *Multi-carrier Digital Communications*. Kluwer/Plenum, 2002. ISBN: 978-0387225753

[5] GOLDSMITH, A. *Wireless Communications*. Artech House, 2005. ISBN: 978-0521837163

[6] CHETTAT, H., SIMOHAMED, L. M., ALGANI, C., et al. Co-simulation-based modeling and performance analysis of hybrid fiber-wireless links. *International Journal of Communication Systems*, 2013, vol. 26, no. 5, p. 583–596. DOI: 10.1002/dac.1361

[7] HOSSAIN, MD. A., TARIQUE, M. Effect of multipath fading and multiple access interference on broadband code division multiple access systems. *International Journal of Communication Systems*, 2012, vol. 25, no. 7, p. 874–886. DOI: 10.1002/dac.1293

[8] BAGHERSALIMI, G. Performance assessment of a wideband code-division multiple access-based radio-over-fibre system with near–far effect: downlink scenario. *IET COM*, 2014, vol. 8, no. 7, p. 1056–1064. DOI: 10.1049/iet-com.2013.0805

[9] PATRA, J. C., MEHER, P. K., CHAKRABORTY, G. Nonlinear channel equalization for wireless communication systems using Legendre neural networks. *Signal Processing*, 2009, vol. 89, no. 5, p. 2251–2262. DOI: 10.1016/j.sigpro.2009.05.004

[10] CHANDRA KUMAR, P., SARATCHANDRAN, P., SUNDARAJAN, N. Minimal radial basis function neural networks for nonlinear channel equalization, *IEEE Proceedings - Vision, Image and Signal Processing*, vol. 147, no. 5, Oct. 2000, p. 428–435. DOI: 10.1049/ip-vis:20000459

[11] NAWAZ, S. J., MOHSIN, S., IKRAM, A. A. Neural network based MIMO-OFDM channel equalizer using comb-type pilot arrangement. In *International Conference on Future Computer and Communication*. Kuala Lumpur (Malaysia), 2009, p. 36–48. DOI: 10.1109/ICFCC.2009.136

[12] PATRA, J. C., POH, W. B., CHAUDHARI, N. S., DAS, A. Nonlinear channel equalization with QAM signal using Chebyshev artificial neural network. In *Proceedings of International Joint Conference on Neural Networks*. Montreal (Canada), 2005, p. 3214–3219. DOI: 10.1109/IJCNN.2005.1556442

[13] RAHMAN, Q. M., IBNKAHLA, M., BAYOUMI, M. Neural network based channel estimation and performance evaluation of a time varying multipath satellite channel. In *Proceedings of the 3rd Annual Communication Networks and Services Research Conference* (*CNSRC'05*). Halifax (Canada), May 2005, p. 74–79. DOI: 10.1109/CNSR.2005.44

[14] DENG JIANPING, SUNDARAJAN, N., SARATCHANDRAN, P. Communication channel equalization using complex-valued minimal radial basis function neural networks. *IEEE Transactions on Neural Networks*, 2002, vol. 13, p. 687–696. DOI: 10.1109/TNN.2002.1000133

[15] PATRA, J. C., CHIN, W. C., MEHER, P. K., CHAKRABORTY, G. Legendre-FLANN-based nonlinear channel equalization in wireless communication system. In *IEEE International Conference on Systems, Man and Cybernetic*. Singapore, 2008, p. 1820–1831. DOI: 10.1109/ICSMC.2008.4811554

[16] DEVELI, I. Application of multilayer perceptron networks to laser diode nonlinearity determination for radio-over-fibre mobile communications. *Microwave and Optical Technology Letters*, 2004, vol. 42, no. 5, p. 425–427. DOI: 10.1002/mop.20325

[17] BAGHERSALIMI, G. A comparative performance study of optical subsystem equalization in OFDM-based and OWDM-based radio-over-fiber systems. In *Proceedings of the 11th International Conference on Telecommunications ConTEL2011*. Graz (Austria), 2011, p. 315–320. ISBN: 978-3-85125-161-6

[18] *IEEE std 802.11g*; Supplement to IEEE standard for information technology telecommunications and information exchange between systems-local and metropolitan area networks specific requirements-part 11: Wireless LAN medium access control (MAC) and physical layer (PHY) specifications; amendment 4: Further higher data rate extension in the 2.4 GHz band. Tech. rep., IEEE, 2003. ISBN : 978-0-7381-6324-6

[19] BOSCH, W., GATTI, G. Measurement and simulation of memory effects in pre-distortion linearizers. *IEEE Transactions on Microwave Theory and Techniques,* 1989, vol. 37, no. 12, p. 1885 to 1890. DOI: 10.1109/22.44098

[20] WAY, W. I., AFRASHTEH, A. Linearity characterization of connectorized laser diodes under microwave intensity modulation by am/am and am/pm measurements. In *IEEE MTT-S International Microwave Symposium Digest*. Baltimore (USA), 1986, vol. 86, no. 1, p. 659–662. DOI: 10.1109/MWSYM.1986.1132274

[21] DEMUTH, H., BEALE, M., HAGAN, M. Neural networks toolbox user's guide for use with matlab 7. The Mathworks Inc, 2006. Available at: http://www.mathworks.com

About the Authors …

Leila SAFARI received M.Sc. degree in Electronics Engineering from the University of Guilan, Rasht, Iran in 2011. Her research interests include neural networks and radio-over-fiber systems.

Gholamreza BAGHERSALIMI (corresponding author) is with the Department of Electrical Engineering, the University of Guilan, Rasht, Iran. He received his B.Sc. degree from Tehran University, Tehran, Iran in 1990, M.Sc. degree from Tarbiat Modarres University, Tehran, Iran in 1994, and Ph.D. degree from the University of Leeds, Leeds, UK in 2006, all in Communication Engineering. His research interests include equalization and synchronization of multicarrier systems, radio-over-fiber networks, free-space optical communications, visible light communications and spread spectrum techniques.

Ali KARAMI is an Associate Professor in the University of Guilan in Iran. He received B.Sc. at Sharif University of Technology, Tehran, in 1992, M.Sc. at Iran University of Science and Technology, Tehran, in 1994 and Ph.D. at Amirkabir University of Technology in 1999, all in Electrical Engineering. His research interests include transient stability, transient energy function method and neural network applications.

Abdolreza KIANI received his M.Sc. degree in Electronics Engineering from the University of Guilan, Rasht, Iran in 2011. His research interests include equalization and radio-over-fiber systems. Now, he is with the Islamic Azad University, Abadan branch.